European Journal of Radiology 121 (2019) 108702

Contents lists available at ScienceDirect

European Journal of Radiology

journal homepage: www.elsevier.com/locate/ejrad

Comparison of image quality between split-filter twin beam dual energy and single energy images in abdominal CT

Zhongfeng Niu[a], Jiao Chen[a], Hong Ren[a], Yang Wang[b], XinWei Tao[b], Kun Zhan[a,*]

[a] Department of Radiology, Sir Run Run Shaw Hospital, Zhejiang University College of Medicine and Sir Run Run Shaw Institute of Clinical Medicine of Zhejiang University, No. 3, East Qingchun Road, Hangzhou, 310016, China

[b] Siemens Healthineers, No. 278, Zhouzhugong Road, Shanghai, 201318, China

ARTICLE INFO

Keywords:
Twin-beam dual-energy
Split-filter
Image quality
Abdominal CT

ABSTRACT

Purpose: To compare the objective and subjective image quality between composed images from split-filter twin beam dual energy (TBDE) and single-energy computed tomography (SECT) in abdominal CT.

Methods: In this prospective study, 103 patients were imaged using TBDE (n = 51) or SECT (n = 52). The CT number and noise were measured for the following six abdominal structures: liver, spleen, fat, muscle, aorta and portal vein. The normalised noise level for the liver was separately measured and compared. The consistency of the SNR and CT number was compared between the two groups. The subjective image quality was evaluated using six aspects in a blinded manner. Cohen's Kappa statistic was used to determine the level of agreement between the two radiologists.

Results: For the objective image quality comparison, the SNR of all structures was higher using TBDE compared to SECT ($p < 0.05$). The CT value for different structures were comparable between the two groups ($p > 0.05$). Among all patient sizes, the noise level for TBDE images was significantly lower (7–17% reduction) compared to the SECT images ($p < 0.01$). Furthermore, noise reduction's magnitude increases with body size. For image quality's subjective evaluation, TBDE images are superior for certain aspects. Cohen's Kappa values (0.7634–0.8460) suggest an adequate level of agreement between the two observers.

Conclusions: TBDE scan mode can yield similar or even better objective and subjective image quality at the same level of radiation than conventional SECT. Quantitatively, TBDE images have a 7–17% reduction in noise, depending on the size of the scanned body regions.

1. Introduction

Dual-energy computed tomography (CT) is now well accepted and widely used in enhanced CT examination. Iodine, which is used as the contrast media, may be accurately quantified based on its energy-dependent changes in attenuation values [1–4]. Many studies have also demonstrated that even for non-enhanced clinical cases, dual-energy CT can be utilised for material characterisation, which could be valid for various clinical applications [5,6].

Dual-energy CT is now commercially available based on various approaches, e.g. dual-source with different energy, high-frequency kV switching and dual-layer detectors [7–9]. However, all these techniques are only available through high-end systems that are not cost-effective for routine examinations. Performing the scan twice at different energy levels could be a much simpler and cheaper approach [10], but its poor temporal resolution strongly restricts its applications. This is because the relative motion between the two scans can easily affect the confidence level of diagnosis [11]. Recently, Siemens Healthcare unveiled a novel, dual-energy acquiring mode with twin-beam or split-filter technique. The dual-energy performance of this method is well recognised [12]. This method of CT introduces a split-filter consisting of equal parts gold and tin (Fig. 1). This novel technique is available on mid-end CT systems, which means it has the potential to be used by a larger population on a more frequent basis.

Compared with dual-source dual-energy imaging, single-source dual-energy can suffer from reduced spectral separation, decreased dose efficiency, and, in some approaches, poorer temporal coherence [13]. This study is to investigate whether TBDE can provide comparable objective and subjective image quality with SECT at the same reference CTDIvol in abdominal scan.

Abbreviations: SE, single-energy; SECT, single-energy CT; TBDE, twin-beam dual-energy; SNR, signal-to-noise Ratio; CTDIvol, CT dose index volume

* Corresponding author.
E-mail address: 3414023@zju.edu.cn (K. Zhan).

https://doi.org/10.1016/j.ejrad.2019.108702
Received 26 April 2019; Received in revised form 23 July 2019; Accepted 12 October 2019

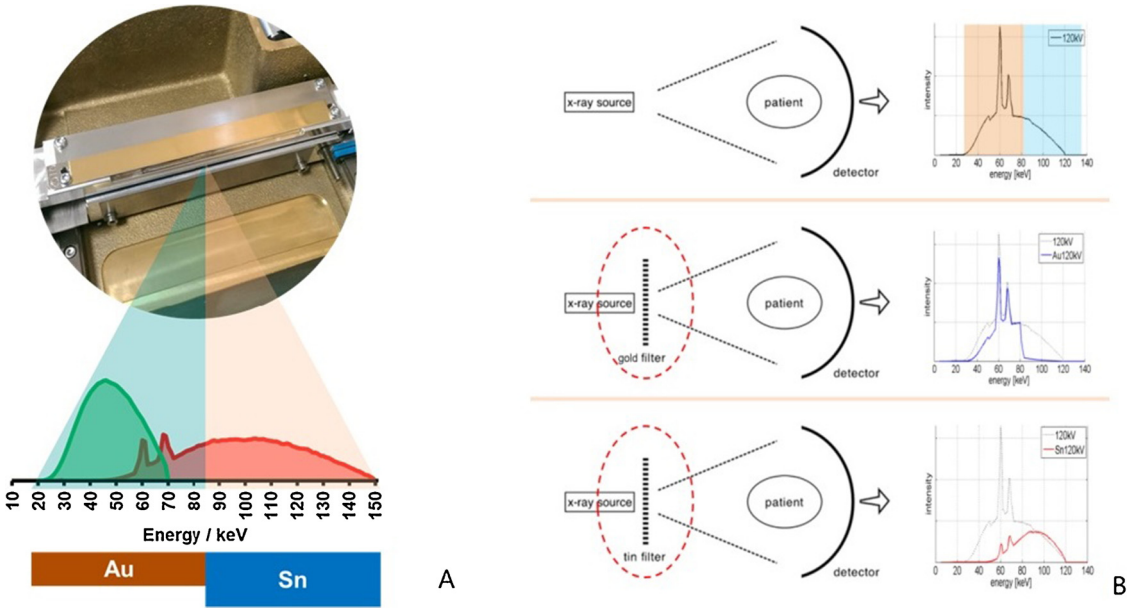

Fig. 1. A schema demonstrates principle of split-filter dual energy.
Description:
1a : The schematic diagram on the left demonstrates the splitting of the x-ray beam into 2 parts. 1b: The first schema shows spectrum without filtration at 120 kV, the second schema shows spectrum after gold filtration with low-energy spectrum left, and the third one shows after tin filtration with high energy spectrum left.

2. Materials and methods

2.1. Study design and patient population

The study population consisted of 103 adult patients (mean age 50.84 ± 11.89 years, 65 women, 38 men) who underwent abdominal CT by SOMATOM go. Top (Siemens Shanghai Medical Equipment Ltd., Shanghai, China, SomarisX VA20) between October and November 2018. This study was approved by the ethics committee. The inclusion criteria for this study is as follows: 1) in good health, 2) older than 18 years of age, 3) willing to undergo abdominal CT scan, 4) did not undergo CT scan within one year and 5) The informed consent document for X-ray examination was read, understood and signed for each patient. The exclusion criteria were as follows: 1) without full capacity for civil conduct, 2) planned to get pregnant within three months, 3) pregnant or breastfeeding and 4) having a metal implant within abdominal region. Patients were randomly assorted into both groups. One hundred and three patients were scanned using either TBDE (n = 51) mode or SECT mode (n = 52). There were no significant differences in gender, age, weight, height and BMI ($p \geq 0.05$, Table 1) between the two groups.

2.2. Scan protocol and image reconstruction

The scan protocol details were listed in Table 2. The scan voltage for the conventional SE scan was set to 120 kV as routine. Reference mAs or CTDIvol were used to standardise the image quality, i.e. when dose modulation is active, similar image quality may be achieved for patients of different sizes. They are determined and calculated by manufacturer. During each scan, Care Dose4D was used as the dose modulation technique for adapting the dose in real time. It automatically modulated the X-ray tube current according to the size and anatomy of each patient. It was always turned on during our study to maintain the desired level of image quality while substantially reducing unnecessary doses of radiation. Of note, the reference tube current–time product had to be set to a very high value in TBDE (354 mAs) to get a same CTDIvol level, because a large portion of the emitted photons are absorbed by the split-filter which is placed in front of the tube output.

The composed images from TBDE were created by a linear blending of low- and high-energy images which derive from the spectral separation by the split-filter. These composed images aim to simulate the attenuation characteristics and image impression of a polychromatic scan at 120 kV. For both SECT and composed images, the same reconstruction parameters were used: 5 mm slice thickness, Br40 kernel and SAFIRE strength3.

Table 1
Characteristic statistic of the population studied.

Patient characteristic	SECT	TBDE	p-value
Gender	M: 20 | F: 31	M: 18 | F: 34	0.7669
Age (yr)	52.92 (29-82)	49.92 (25-75)	0.2054
Height (cm)	162.24 (149-183)	163.25 (145-178)	0.5164
Weight (kg)	61.18 (35-86)	62.13 (47-82)	0.6375
BMI	23.14 (15.6-33.3)	23.25 (17.8-29.6)	0.85

Table 2
Scan parameters of single-energy (SECT) and twin-beam dual-energy (TBDE) protocols used for this study.

Scan parameter	SECT	TBDE
Voltage (kV)	120	120 AuSn
Detector collimation (mm)	64 × 0.6	64 × 0.6
Rotation time (s)	0.5	0.33
Pitch	0.8	0.35
Reference mAs	110	354
Reference CTDIvol (mGy)	9.9	9.912
Care Dose4D & Care kV	Care Dose 4D on & Manual kV	Care Dose 4D on & Manual kV

2.3. Objective image quality evaluation

2.3.1. CT value and SNR

The CT attenuation (in Hounsfield Units) of the parenchyma of liver, spleen, subcutaneous fat, muscle, aorta and portal vein were measured by two radiologists (Z.K and R.H). The measurement was performed by placing circular regions of interest (ROI) on the 5-mm axial images of

all 103 CT data sets. All measurements were performed three times and the mean values were calculated. For liver, 3 cm^2 ROIs were placed in a uniform-density region on the left robe, the right anterior lobe and right posterior lobe. For fat, 2 cm^2 ROIs were measured at the level of the umbilicus. For muscle, 3.0 cm^2 ROI were placed above the level of the hip joint. For the aorta, a 1 cm^2 ROI was placed on three continuous levels of origin on the celiac trunk. For the portal vein, three 0.5 cm^2 ROIs were placed on the portal stem vein. The SNR of every structure is calculated as the average CT number/SD and compared using an independent sample *t*-test.

2.3.2. Noise level

To avoid measurement error, the liver was selected as a surrogate of noise level, since it is the largest organ in abdominal region with good uniformity and easy to place ROIs. Meanwhile, we chose the slices of the right branch of hepatic portal vein for different patients.

Since each individual image was obtained with different dose, in order to have a more robust quantitative analysis, the normalised noise was used. It is calculated as $\sigma^2 \bullet CTDIvol$. CTDIvol represented the actual CTDI of the slice, while the average noise is calculated by $\sigma = \sqrt{\sum_{n=1}^{3} \sigma_n^2/3}$, where σ_n are standard deviations of three measured ROIs. The actual dose (CTDIvol) of the measured slice was calculated by converting the effective mAs with the dose factor provided in user manual. Then the normalised noise is calculated by $\sigma^2 \bullet CTDIvol$. Since the patient size may also affects noise performance, we also calculated 'equivalent diameter', $D = \sqrt{D_1 \bullet D_2}$, of the measured slices, where D_1 is patient diameter in vertical direction and D_2 is patient width in horizontal direction. Finally, noise level was compared between the two groups while taking patient size into consideration.

Two examples of selected images and how they were measured are shown in Fig. 2. The measured results for evaluating objective image quality are summarised in Table 3. All measurements were performed directly on the scanner interface with the integrated Syngo. View & Go. (Siemens Shanghai Medical Equipment Ltd., Shanghai, China, SomarisX VA20)

2.4. Subjective image quality evaluation

Full image data sets from both SECT and TBDE were evaluated independently by two radiologists (C.J, and Z.F), with 7 and 10 years of experience in abdominal CT imaging, respectively. All data sets were randomised and the two readers were blinded to acquisition parameters. All abdominal CT image data sets were viewed side-by-side on a PACS (EWord, China, Version 2018.1226,1200). Standard abdominal window setting (window width, 300 HU; window level, 40 HU) was used for image assessment, but radiologists were also allowed to change the window level and width as per their comfort level during the assessment.

Table 3
Summary of the measurements on the selected images in Fig. 2.

Measured values	SECT	TBDE
Effective mAs	58	179
Actual CTDIvol (mGy)	58·9.0/100 = 5.220	179·2.8/100 = 5.012
Patient size, D (cm)	√(20.26 * 27.22) = 23.6	√(20.01 * 26.39) = 23.09
Averaged CT value of liver (HU)	(66 + 69 + 70)/3 = 68.3	(66 + 66 + 67)/3 = 66.3
Averaged noise in liver (HU)	$\sqrt{(11^2 + 10^2 + 10^2)} = 10.34$	$\sqrt{(9^2 + 8^2 + 8^2)} = 8.35$

Subjective assessment was performed based on the following aspects: noise, subjective contrast, sharpness, small structure, artefact and diagnostic confidence according to the European Guidelines on Quality Criteria [14] (Table 4). Generally, a score of 1 represented the best rating, while a score of 5 represented the worst rating. Since the rating score is subjective, we considered the ratings from two readers consistent if the difference is less than 1 point during our statistical analysis.

2.5. Statistical analysis

Dunnett's *t*-test was used to analyse age, height, weight and BMI, while the Chi-Square test was used to determine whether the two groups had equal distribution of patient gender. For comparing dose and SNR, an independent samples *t*-test was used after confirming normal distribution of data. The level of statistical significance was set at $p < 0.05$. For analysing objective image quality, performance, dose and noise, a 2-D version of the two-sample Kolmogorov–Smirnov (K–S) test was used since these values strongly depend upon the size of the patient. For analysing subjective image quality, e.g. rating scores from examiners, the Mann–Whitney U test was used. For checking the level of agreement between the two observers, Cohen's Kappa statistic was used. All statistical analyses were performed with SPSS V19.0 (IBM, Armonk, New York) except for the 2-D two-sample K–S test, which was performed manually using the equations described in the reference [15].

3. Results

3.1. Objective image quality – patient size and dose

For abdominal scans, the actual CTDIvol for SECT and TBDE are 6.40 ± 1.22 mGy and 6.62 ± 1.04 mGy, respectively, ($p = 0.32$). The mean effective doses for SECT and TBDE were 4.23mSv and 4.6mSv, repectively, and there was no significance differences between both groups ($p = 0.09$).

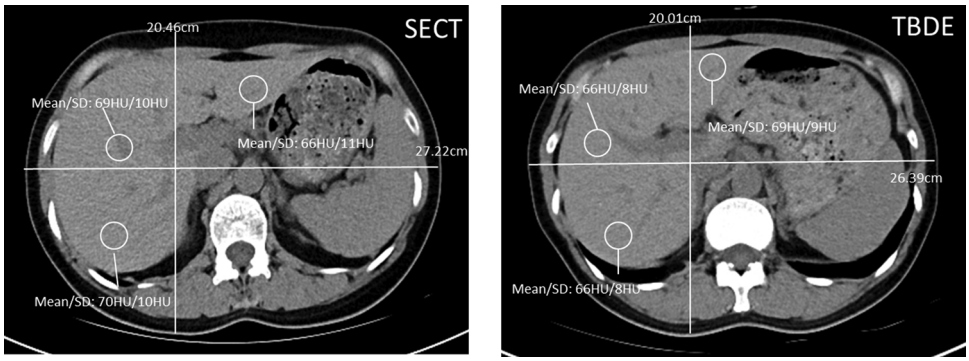

Fig. 2. Measurement of images.
Description:
Examples of selected images for both SECT (left) and TBDE (right), showing the anatomy and how they are measured. mAs in left image: 58, mAs in right image:179

Table 4
Summary of the criteria of rating used in this paper.

Rating	1	2	3	4	5
Noise	Minimal	Less than average	average	Above average	Unacceptable
Subjective contrast	Excellent	Above average	acceptable	suboptimal	Very poor
Sharpness	Excellent	Above-average sharpness	Average	Below average	Blurry
Small structure	excellent	above average	acceptable	suboptimal	unacceptable
Artifact	No artifacts	Minor artifacts not interfering with diagnostic decision making	Major artifacts affecting visualization of major structures, diagnosis still possible	Artifacts affecting diagnostic information	–
Diagnostic confidence	Completely confident	Probably confident	Confident only for a limited clinical situation, such as calcified or large lesions	Poor confidence	Nondiagnostic examination

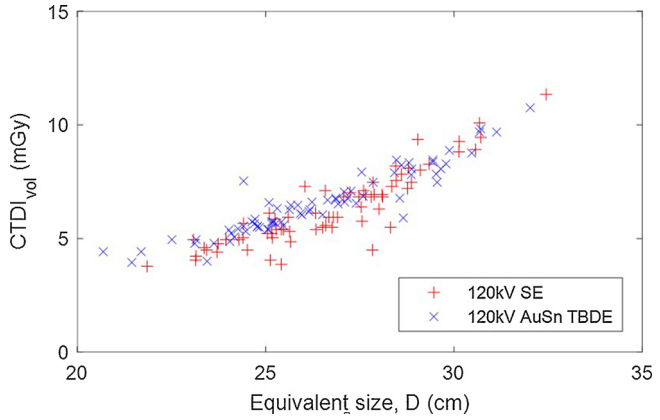

Fig. 3. Comparison of dose between two groups.
Description:
Distribution of dose against patient equivalent size for both SECT and TBDE with D_{KS} = 1.3686 in 2-D K–S test.

For the studied liver slices, the actual CTDIvol of the SECT and TBDE scans showed no significant difference according to the 2-D K–S test, with D_{KS} = 1.3686. (Fig. 3)

3.2. Objective image quality – patient size and normalised noise

Significantly lower noise levels were detected in the TBDE images compared to SECT images was found using the 2-D K–S for 'normalised noise − patient size' distribution with D_{KS} = 1.8749. Furthermore, the noise reduction's magnitude increases with body size as shown in Fig. 4.

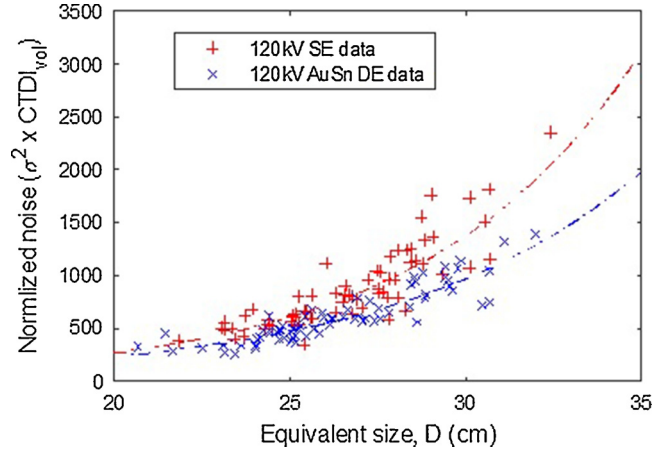

Fig. 4. Comparison of dose normalized noise between two groups.
Description:
The distribution of normalized noise against patient equivalent size for both SECT and TBDE, with best-fitted exponent curves shown as dash dot lines.

Table 5
SNR in each structure.

Measured organ	TBDE	SECT	p-value
Liver	6.8	6.08	0.001
Aorta	4.57	4.15	0.001
Spleen	6.2	5.5	0
Fat	−12.75	−11.03	0
Muscle	5.87	5.07	0.002
Portal Vein	4.47	3.85	0

Table 6
CT attenuation values (HU values) measured for different organs.

Measured organ	SECT	TBDE	p-value
Liver	67.03 ± 5.83	63.76 ± 8.71	0.0277(> 0.1 with 2D K-S test
Aorta	47.20 ± 3.36	46.18 ± 3.65	0.142
Spleen	55.95 ± 3.40	53.31 ± 2.45	< 0.0001
Fat	−105.59 ± 5.68	−102.18 ± 3.65	0.0004
Muscle	53.52 ± 4.58	53.36 ± 4.25	0.8509
Portal Vein	43.90 ± 4.75	43.87 ± 4.05	0.9665

3.3. Objective image quality – SNR and CT value

SNR of the composed images using TBDE was significantly higher compared to SECT in all six structures as shown in Table 5. In Table 6, the mean HU values and the variances for all measured organs were listed. Although minor differences in HU were found in spleen and fat, the CT values were comparable in the muscle and portal vein. For liver, since the HU value is related to fat content or patient BMI, the 2-D distribution of liver HU values against patient BMI was checked. These results suggest these two distributions from SECT and TBDE are comparable with p > 0.1 (Fig. 5).

3.4. Subjective image quality – inter-observer agreement

The ratings from two observers were compared to assess the image quality subjectively. Cohen's Kappa values ranging from 0.7634 to 0.8460 suggest a good level of agreement was obtained for all six aspects used to assess subjective image quality. Since the subjective image quality rating has some randomness and variance, a difference in rating of 1 point is still considered as being 'in agreement'.

3.5. Subjective image quality – SECT vs. TBDE

Since the ratings from the two observers were consistent, we averaged the scores before comparing the subjective image quality between the SECT and TBDE images. In all aspects regarding subjective image quality, TBDE images had better quality compared SECT images, although the improvement was moderate. Detailed distributions of average rating scores are listed in Table 7.

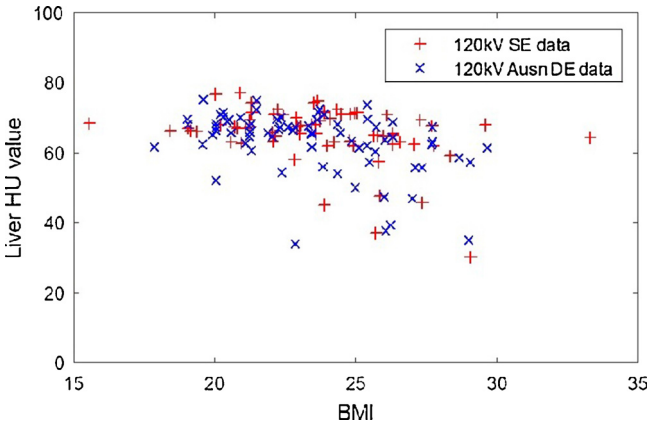

Fig. 5. Liver HU comparison with 2-D K–S test.
Description:
Distribution of liver HU value against patient BMI for both SECT and TBDE with D_{KS} = 1.2586 in 2-D K–S test.

4. Discussion

Our main findings for this study were as follows: 1) CT numbers from TBDE and SECT are comparable in six abdominal structures. Meanwhile, TBDE has better SNR compared to SECT under the same CTDIvol, which is in accordance with subjective image quality evaluation. 2) These findings were accompanied by a significantly lower noise level in the liver (up to 17% reduction) using TBDE. The magnitude of this reduction increases with body size.

We attribute the significant optimisation in image quality to the use of spectral shaping, primarily due to the tin filter. This filter absorbs low-energy photons, thus narrowing and shifting the polychromatic x-ray spectrum towards higher energies. In other words, low-energy photons, which are usually responsible for higher noise and lower CT image quality due to absorption or scattering phenomena [16], are filtered out from the detector signal. As a result, TBDE exposes patients to similar levels of radiation while decreasing image noise and providing better image quality compared to conventional SECT. Some studies have shown better dose optimisation in SECT [13,17]. In a phantom study, Euler et al found size-specific dose estimate of TBDE is 17% lower than that of SECT while the objective image noise is similar [13], which is consistent with our study. Another study showed a noise reduction of 18% using an identical TBDE technique [17]. Unlike previous studies [12,13], we are doing a prospective study, where the dose and expectations of image quality are strictly from the protocol setting at the beginning of the study. In an *in vivo* study, Euler et al. measured SNR and CNR on the liver, hilum and abdominal aorta [12]. Our study examined six structures, which is more detailed. Previous studies usually included DLP analyses when comparing dose [13,17]. While we believe that the overall DLP could strongly depend on the diagnostic purpose and scan range, the variance could be too large to indicate any difference. Instead, we used actual CTDIvol from same reference CTDIvol after automatic dose modulation (CareDose 4D) for patients of different sizes. In addition to previous studies, our results show that the dose optimisation could vary according to the size of scanned patient. For patients with an equivalent diameter of 20 cm, the noise reduction is 7%, while, noise reduction is up to 17% for those with patients with an equivalent diameter of 33 cm.

Table 7
Averaged subjective image quality ratings from two observers.

Noise										
	1	1.5	2	2.5	3	3.5	4	4.5	5	p-value
SECT	–	–	3.90%	15.70%	37.20%	41.20%	2.00%	–	–	0.0023
TBDE	–	1.90%	11.60%	26.90%	42.30%	15.40%	1.90%	–	–	
Subjective Contrast										
	1	1.5	2	2.5	3	3.5	4	4.5	5	p-value
SECT	–	–	23.50%	23.50%	43.20%	7.80%	2.00%	–	–	0.0153
TBDE	–	1.90%	32.70%	40.40%	19.20%	5.80%	–	–	–	
Artifact										
	1	1.5	2	2.5	3	3.5	4	4.5	5	p-value
SECT	–	5.90%	41.20%	43.10%	7.80%	2.00%	–	–	–	0.0529
TBDE	–	15.40%	48.10%	30.80%	5.80%	–	–	–	–	
Small structure										
	1	1.5	2	2.5	3	3.5	4	4.5	5	p-value
SECT	–	–	3.90%	15.70%	37.20%	41.20%	2.00%	–	–	0.041
TBDE	–	3.90%	30.80%	44.20%	9.60%	9.60%	1.90%	–	–	
Sharpness										
	1	1.5	2	2.5	3	3.5	4	4.5	5	p-value
SECT	–	2.00%	29.40%	33.30%	19.60%	15.70%	–	–	–	0.0547
TBDE	–	1.90%	48.10%	26.90%	15.40%	7.70%	–	–	–	
Diagnostic confidence										
	1	1.5	2	2.5	3	3.5	4	4.5	5	p-value
SECT	–	2.00%	37.30%	33.30%	21.60%	5.90%	–	–	–	0.0206
TBDE	–	3.90%	53.80%	32.70%	7.70%	1.90%	–	–	–	

We chose the abdominal region for this study because it contains different organs with HU values that are sensitive to the spectra used for scanning. The absolute HU values for different organs may also provide diagnostic information in abdominal CT. For four of the six measured structures, namely the liver, aorta, muscle and portal vein, we obtained a very consistent HU values from both SECT and TBDE scans. For spleen and fat, the difference in HU values obtained from both scans is significant ($p < 0.001$). This may be due to the fact that fat is measured close to the skin, and beam-hardening artefacts might affect the image quality. For the spleen, it is located just behind the lung, and the difference in attenuation for the two organs may cause this difference in HU values. Also, the beam-hardening artefact from ribs might also be a reason. Although the HU values for these two organs are statistically different, the absolute differences are only 2.64 for spleen and 3.41 for fat. The importance of obtaining accurate HU values would be recognised more, since the quantitative information from CT image is now heavily used i.e. in radiometric and deep learning. This also means that images from TBDE scan could also provide input for computer-aided diagnosis. A number of studies comparing the performance between TBDE and other dual-energy techniques have demonstrated the utility of extra dual-energy information provided by TBDE [18–21]. According to the intrinsic characteristics of dual-energy CT, more robust tissue analysis and material quantification are feasible [21], and richer clinical information could be provided for diagnosis.

Two observers had a high level of agreement with each other on all subjective image quality ratings, and the averaged ratings from TBDE scans had similar or lower scores than those from SE scans. Also, the observers subjectively determined that TBDE images had significant lower noise compared to SE images ($p < 0.01$), which is consistent with our quantitative objective measurements. This positive result demonstrated that using TBDE instead of SE for abdominal CT can provide equivalent or even superior image quality for daily diagnosis using the same dose of radiation. Besides the benefits mentioned above, TBDE offers more possibilities, more post-processing approaches and clinical information without repeating the scan. For example, images from patients with metal implants could be post-processed with high keV to reduce metal artefacts and material decomposition could be used for patients with kidney stones.

Our study also has some limitations. First, although our studied populations have a fairly equal distribution comparing with each other, but the whole population tend to have a big average age and standard BMI. Secondly, no paediatric or extreme obese case is covered. At last, some important details, such as calcification, metal artefact or other organs have not been assessed.

In conclusion, our prospective study demonstrated that compared to conventional SE scans, TBDE is a novel dual-energy acquiring technique that will provide comparable image quality with less noise. It suggests that TBDE has potential to be used for routine abdominal scans without compromising diagnostic efficiency. Together with its low cost and ability to provide more clinical information, TBDE is a promising, dual-energy acquisition technique that can be used by wider communities in daily clinical practice in lieu of SE examinations.

Declaration of Competing Interest

None.

References

[1] A. Graser, T.R. Johnson, E.M. Hecht, et al., Dual-energy CT in patients suspected of having renal masses: can virtual non enhanced images replace true non enhanced images? Radiology 252 (2009) 433–440, https://doi.org/10.1007/s10140-013-1141-9.

[2] M. Toepker, T. Moritz, B. Krauss, et al., Virtual non-contrast in second-generation, dual-energy computed tomography: reliability of attenuation values, Eur. J. Radiol. 81 (2012) e398–e405, https://doi.org/10.1016/j.ejrad.2011.12.011.

[3] T. Barrett, D.J. Bowden, N. Shaida, et al., Virtual unenhanced second generation dual-source CT of the liver: is it time to discard the conventional unenhanced phase? Eur. J. Radiol. 81 (2012) 1438–1445, https://doi.org/10.1016/j.ejrad.2011.03.042.

[4] J. Baxa, A. Vondrakova, T. Matouskova, et al., Dual-phase dual-energy CT in patients with lung cancer: assessment of the additional value of iodine quantification in lymph node therapy response, Eur. Radiol. 24 (2014) 1981–1988, https://doi.org/10.1007/s00330-014-3223-9.

[5] K.N. Glazebrook, L.S. Guimaraes, N.S. Murthy, et al., Identification of intra articular and peri-articular uric acid crystals with dual-energy CT: initial evaluation, Radiology 261 (2011) 516–524, https://doi.org/10.1016/j.yrad.2011.12.012.

[6] Y. Ju, A. Liu, Y. Dong, et al., The value of nonenhanced single-source dual-energy CT for differentiating metastases from adenoma in adrenal glands, Acad. Radiol. 22 (2015) 834–839, https://doi.org/10.1016/j.acra.2015.03.004.

[7] W.A. Kalender, W.H. Perman, J.R. Vetter, et al., Evaluation of a prototype dual-energy computed tomographic apparatus. 1, Phantom Stud. Med Phys. 13 (1986) 334–339.

[8] R. Carmi, G. Naveh, A. Altman, Material separation with dual-layer CT, IEEE Nucl. Sci. Symp. Conf. Rec. 4 (2005) 1876–1878, https://doi.org/10.1118/1.595958.

[9] C.H. McCollough, S. Leng, L. Yu, et al., Dual- and multi-energy CT: principles, technical approaches and clinical applications, Radiology 276 (2015) 637–653, https://doi.org/10.1148/radiol.2015142631.

[10] S. Leng, M. Shiung, S. Ai, et al., Feasibility of discriminating uric acid from non-uric acid renal stones using consecutive spatially registered low- and high-energy scans obtained on a conventional CT scanner, AJR Am. J. Roentgenol. 204 (2015) 92–97, https://doi.org/10.1016/j.juro.2015.07.037.

[11] Ibrahim el-SH, J.G. Cernigliaro, R.A. Pooley, et al., Motion artifacts in kidney Stone imaging using single-source and dual-source dual-energy CT scanners: a phantom study, Abdom. Imaging 40 (2015) 3161–3167, https://doi.org/10.1007/s00261-015-0530-9.

[12] N. Kaemmerer, M. Brand, M. Hammon, et al., Dual-energy computed tomography angiography of the head and neck with single-source computed tomography: a new technical (Split filter) approach for bone removal, Invest. Radiol. 51 (2016) 618–623, https://doi.org/10.1097/rli.0000000000000290.

[13] A. Euler, A. Parakh, A.L. Falkowski, et al., Initial results of a single-source dual-energy computed tomography technique using a split-filter: assessment of image quality, radiation dose, and accuracy of dual-energy applications in an in vitro and in vivo study, Invest. Radiol. 51 (2016) 491–498, https://doi.org/10.1097/rli.0000000000000257.

[14] M. Leonardi, G. Bongartz, D.J. Geleijns, et al., European guidelines on quality criteria for computed tomography, European Commission, (1999) 17-14 https://ci.nii.ac.jp/naid/10012926527.

[15] G. Fasano, A. Franceschini, A multidimensional version of the Kolmogorov–Smirnov test, Mon. Not. R. Astron. Soc. 225 (1) (1987) 155–170, https://doi.org/10.1093/mnras/225.1.155.

[16] B. Krauss, K.L. Grant, B.T. Schmidt, et al., The importance of spectral separation: an assessment of dual-energy spectral separation for quantitative ability and dose efficiency, Invest. Radiol. 50 (2015) 114–118, https://doi.org/10.1097/rli.0000000000000109.

[17] A. Euler, M.M. Obmann, Z. Szucs-Farkas, et al., Comparison of image quality and radiation dose between split-filter dual-energy images and single-energy images in a single-source abdominal CT, Eur. Radiol. 28 (2018) 3405–3412, https://doi.org/10.1007/s00330-018-5338-x.

[18] I.P. Almeida, L.E. Schyns, M.C. Öllers, et al., Dual-energy CT quantitative imaging: a comparison study between twin-beam and dual-source CT scanners, Med. Phys. 44 (2017) 171–179, https://doi.org/10.1002/mp.13066.

[19] M.C. Jacobsen, D. Schellingerhout, C.A. Wood, et al., Inter manufacturer comparison of dual-energy CT iodine quantification and monochromatic attenuation: a phantom study, Radiology 287 (2018) 224–234, https://doi.org/10.1148/radiol.2017170896.

[20] M.S. May, M. Wiesmueller, R. Heiss, et al., Comparison of dual- and single-source dual-energy CT in head and neck imaging, Eur. Radiol. 29 (8) (2019) 4207–4214, https://doi.org/10.1007/s00330-018-5762-y.

[21] M.M. Obmann, V. Kelsh, A. Cosentino, et al., Interscanner and intrascanner comparison of virtual unenhanced attenuation values derived from twin beam dual-energy and dual-source, dual-energy computed tomography, Invest. Radiol. 54 (1) (2019) 1–6, https://doi.org/10.1097/rli.0000000000000501.